Steel and Composite Structures, *Vol. 36, No. 1 (2020) 31-45*
DOI: https://doi.org/10.12989/scs.2020.36.1.031

Structural damage identification using an iterative two-stage method combining a modal energy based index with the BAS algorithm

Shuqing Wang[1a], Yufeng Jiang[1b], Mingqiang Xu*[1], Yingchao Li[2c] and Zhixiong Li[1d]

[1]Shandong Provincial Key Laboratory of Ocean Engineering, Ocean University of China, 238 Songling Road, Qingdao, Shangdong, China
[2]College of Civil Engineering, Ludong University, 186 Hongqi Middle Road, Yantai, Shangdong, China

(*Received September 10, 2019, Revised June 8, 2020, Accepted June 24, 2020*)

Abstract. The purpose of this study is to develop an effective iterative two-stage method (ITSM) for structural damage identification of offshore platform structures. In each iteration, a new damage index, Modal Energy-Based Damage Index (MEBI), is proposed to help effectively locate the potential damage elements in the first stage. Then, in the second stage, the beetle antenna search (BAS) algorithm is used to estimate the damage severity of these elements. Compared with the well-known particle swarm optimization (PSO) algorithm and genetic algorithm (GA), this algorithm has lower computational cost. A modal energy based objective function for the optimization process is proposed. Using numerical and experimental data, the efficiency and accuracy of the ITSM are studied. The effects of measurement noise and spatial incompleteness of mode shape are both considered. All the obtained results show that under these influences, the ITSM can accurately identify the true location and severity of damage. The results also show that the objective function based on modal energy is most suitable for the ITSM compared with that based on flexibility and weighted natural frequency-mode shape.

Keywords: damage identification; modal energy; beetle antennae search; iterative two-stage method; objective function; noise robustness

1. Introduction

Large-scale civil engineering structures, such as bridges, offshore platforms and wind turbines, usually work in a harsh environment and are under various external loadings. During their service lifespan, structural damages are continuously accumulated. To detect potential damages and further ensure structural safety, damage detection of civil engineering structures in a timely fashion becomes an inevitable scheme (Alamdari *et al.* 2015, Oliveira *et al.* 2018, Chaabane *et al.* 2019, Wang *et al.* 2020). During the past decades, the vibration-based damage detection technique has received considerable attention. The basic idea behind this technique is that the physical properties can alter the dynamic characteristics of the structure, such as natural frequencies, modal damping ratios and mode shapes. In return, these changes can be utilized to reflect the damage state of the structure.

The generalized damage identification process can be divided into four levels. Level 1: determination that damage is present in the structure; Level 2: prediction of the location of the damage; Level 3: estimation of the severity of the damage; and Level 4: prediction of the remaining service life of the structure. In recent years, more and more attention has been paid to Levels 2 and 3 to develop damage localization and quantification methods, which broadly fall into two categories. The first category locates and estimates the severity of damage simultaneously. The principle is to construct a relationship between the location and severity of damage, and a special algorithm is usually used to it. For example, Li *et al.* (2007) and Wang *et al.* (2009) both extended the cross modal strain energy method (Hu *et al.* 2006) to perform damage localization and quantification simultaneously. The over-determined equations were formed and solved based on different hypotheses (Xu and Wang 2017, Wang *et al.* 2019). Similar work has been done by Shi *et al.* (1998).

Another category is the two-stage method (TSM). The basic idea is that one algorithm is applied for damage localization in the first stage and the other is implemented for damage quantification in the second stage after the damage location has been approximately predicted. Usually, the combination of a modal strain energy-based index (MSEBI) and an optimization algorithm is focused. To illustrate, Srinivas *et al.* (2011) proposed a multi-stage approach for structural damage identification using the change ratio of MSE (MSECR) and the genetic algorithm (GA). This approach was found very useful for identifying the location and severity of damage on large-scale structure

*Corresponding author, Ph.D.
E-mail: xumingqiang@stu.ouc.edu.cn
[a]Professor
E-mail: shuqing@ouc.edu.cn
[b]Ph.D. Student
E-mail: jiangyf0120@163.com
[c]Ph.D.
E-mail: yingchao.ouc@163.com
[d]Professor
E-mail: zhixiong_li@uow.edu.au

http://www.techno-press.org/?journal=scs&subpage=8
ISSN: 1229-9367 (Print), 1598-6233 (Online)

with sufficient accuracy. Seyedpoor (2012) proposed a TSM for structural damage detection by using a MSEBI and the particle swarm optimization (PSO) algorithm. Numerical results indicated that the combination of the MSEBI and the PSO can provide a reliable tool for accurate damage identification. Similar work was further done by Kaveh and Zolghadr (2017). Moreover, Vo-Duy *et al.* (2016) improved the differential evolution algorithm with regard to the problem of the computational cost. By combining it with the MSECR method, they successfully detected the damage in a plate-like structure. Satisfactory results were also obtained by Dinh-Cong *et al.* (2019b) by using the Jaya algorithm. Some other valuable work was done by (Kang *et al.* 2012, Tang *et al.* 2013, Shirazi *et al.* 2014, Cha and Buyukozturk 2015, Casciati and Elia 2017, Nobahari *et al.* 2017, Ghiasi and Ghasemi 2018, Tiachacht *et al.* 2018, Dinh-Cong *et al.* 2018).

One of the most remarkable merits of the TSM is that by excluding some healthy elements by the damage localization index, the search space of the optimization algorithm in the second stage is narrowed and then the speed and precision of the optimization process are improved. From this point of view, the feasibility of the TSM for damage detection heavily relies on the damage localization index that defines the optimization space. Usually, the index is constructed by the modal or physical parameters of the structure, which is closely related to the severity of damage of each structural member. Because the damage severity is unknown in prior, a common practice is to construct an approximate damage index, in which the severity of damage of each member is roughly pre-estimated. For example, in order to construct the MSEBI, it is assumed that the severity of damage of each element is zero in Refs. Srinivas *et al.* (2011), Seyedpoor (2012), Vo-Duy *et al.* (2016), Kaveh and Zolghadr (2017), Dinh-Cong *et al.* (2019b). However, this assumption would lead to some uncertainties in damage localization or even in damage quantification. In fact, the damage identification by using the TSM is a typical cyclical procedure. More specifically, the damage severity can be estimated by the optimization algorithm if the damage location is approximately predicted. In return, the damage index should be further updated for re-localization if the severity of damage is acquired. To address this problem, Xu *et al.* (2019) proposed an ITSM for damage detection. In each iteration an iterative MSED indicator was formulated to locate damage, and afterwards the multi-objective PSO algorithm was used to estimate its severity. Iteration continues by successively updating the iterative MSED indicator via the estimated severity.

Another important factor determining the success of the TSM is the optimization process, in which the selection of objective function is of significance because it guides the search of the true damage severity. Modal parameters based objective functions, such as natural frequencies, mode shapes, modal flexibilities, and their combinations, were widely used (Pandey and Biswas 1994, Perera *et al.* 2009, Meruane and Heylen 2011, Villalba and Laier 2012, Shabbir and Omenzetter 2016, Frigui *et al.* 2018).

In this study, an ITSM is developed for structural damage identification. In each iteration, the newly proposed MEBI is used to help locate the potential damaged elements in the first stage. Then damage severity of these elements is estimated in the second stage by minimizing an objective function by the BAS algorithm. A damage-energy objective function that was rarely used for structural damage identification is proposed. The paper is arranged as follows. In section 2, the MEBI for damage localization and the BAS algorithm for damage severity estimation are introduced as the theoretical backgrounds. Then the ITSM combining the MEBI with the BAS algorithm is proposed for damage identification. A numerical and an experimental examples are adopted to demonstrate its effectiveness of the ITSM in sections 3 and 4, respectively. Conclusions are finally drawn in section 5.

2. Iterative two-stage method for structural damage identification

2.1 MEBI for damage localization

To apply the MEBI, an accurate finite element model (FEM) accurately representing the dynamic features of the undamaged structure must be firstly established as a baseline model. Assuming the mass and stiffness distributions of the baseline model have been known, the mass and stiffness matrices can be constructed and the vibration characteristics of the baseline model can be obtained by solving the corresponding eigenvalue problem

$$(\mathbf{K}-\omega_i^2\mathbf{M})\boldsymbol{\phi}_i=\mathbf{0} \tag{1}$$

where ω_i and $\boldsymbol{\phi}_i$ are the *i*-th natural frequency and mode shape; $\mathbf{K}$ and $\mathbf{M}$ are the stiffness and mass matrices overall structural system of the baseline model, respectively. The MSE of the overall structural system is given by

$$MSE_i=\frac{1}{2}\boldsymbol{\phi}_i^T\mathbf{K}\boldsymbol{\phi}_i \tag{2}$$

Likewise, the MSE of the *j*-th element can be expressed as

$$MSE_{ij}=\frac{1}{2}\boldsymbol{\phi}_i^T\mathbf{K}_j\boldsymbol{\phi}_i \tag{3}$$

where $\mathbf{K}_j$ is the stiffness matrix of the *j*-th element in the global coordinate. Then the MSE ratio (MSER) of the *j*-th element to the overall structural system can be defined as

$$FS_{ij}=MSE_{ij}/MSE_i \tag{4}$$

Throughout this study, the superscript * is used to represent the parameters associated with the damaged structure. Then for the damaged structure, the MSER can be similarly written as

$$FS_{ij}^*=MSE_{ij}^*/MSE_i^* \tag{5}$$

where MSE_i^* and MSE_{ij}^* are the *i*-th MSEs of the overall structural system and *j*-th element, respectively and given by

$$MSE_i^* = \frac{1}{2}\boldsymbol{\phi}_i^{*T}\mathbf{K}^*\boldsymbol{\phi}_i^* \tag{6}$$

$$MSE_{ij}^* = \frac{1}{2}\boldsymbol{\phi}_i^{*T}\mathbf{K}_j^*\boldsymbol{\phi}_i^* \tag{7}$$

The scaled type of mode shapes $\boldsymbol{\phi}_i$ and $\boldsymbol{\phi}_i^*$ is usually required to be identical but not necessary to be mass-normalized.

It is widely accepted that the MSE-based method is an effective tool to locate damage on 1/2/3D structures (Stubbs *et al.* 1995, Cornwell *et al.* 1999, Wang and Xu 2019). However, many scholars argued that the structural modal kinetic energy (MKE) is also an effective tool for damage localization (Dinh-Cong *et al.* 2019a, c). Similar to the MSER, the MKE ratio (MKER) of the j-th element associated with i-th mode of the baseline model and the damaged structures are respectively defined as

$$FK_{ij} = \frac{MKE_{ij}}{MKE_i} = \frac{\frac{1}{2}\omega_i^2\boldsymbol{\phi}_i^T\mathbf{M}_j\boldsymbol{\phi}_i}{\frac{1}{2}\omega_i^2\boldsymbol{\phi}_i^T\mathbf{M}\boldsymbol{\phi}_i} = \frac{\boldsymbol{\phi}_i^T\mathbf{M}_j\boldsymbol{\phi}_i}{\boldsymbol{\phi}_i^T\mathbf{M}\boldsymbol{\phi}_i} \tag{8}$$

$$FK_{ij}^* = \frac{MKE_{ij}^*}{MKE_i^*} = \frac{\frac{1}{2}\omega_i^{*2}\boldsymbol{\phi}_i^{*T}\mathbf{M}_j^*\boldsymbol{\phi}_i^*}{\frac{1}{2}\omega_i^{*2}\boldsymbol{\phi}_i^{*T}\mathbf{M}^*\boldsymbol{\phi}_i^*} = \frac{\boldsymbol{\phi}_i^{*T}\mathbf{M}_j^*\boldsymbol{\phi}_i^*}{\boldsymbol{\phi}_i^{*T}\mathbf{M}^*\boldsymbol{\phi}_i^*} \tag{9}$$

It is assumed that the damage in a small region has a significant influence on the MSER and MKER of the damaged members but little influence on the healthy ones. Thus the change of the MSER and MKER named modal energy based index (MEBI) due to the damage is defined as the damage localization index used in this study.

$$MEBI_{ij} = FS_{ij}^* + FK_{ij}^* - FS_{ij} - FK_{ij} \tag{10}$$

Introduce a purely geometric stiffness $\mathbf{K}_{j0}$

$$\mathbf{K}_j = E_j\mathbf{K}_{j0}, \mathbf{K}_j^* = E_j^*\mathbf{K}_{j0} \tag{11}$$

where E_j and E_j^* are the elasticity or torsion moduli of the j-th element of the healthy and damaged structures, respectively. Besides, it is assumed that the structural damage can be simulated as a reduction of stiffness (Pandey *et al.* 1991, Dessi and Camerlengo 2015) of the damaged element and this reduction can be achieved by modifying its modulus of elasticity, i.e.,

$$E_j^* = (1-\alpha_j)E_j, j = 1,2,\dots,N_e \tag{12}$$

where $\alpha_j \in [0,1]$ is the severity of damage of the j-th element.

Substituting Eqs. (4)-(5), (8)-(9), (11)-(12) into Eq. (10) and considering $\mathbf{K} = \sum_{j=1}^{N_e}\mathbf{K}_j$ and $\mathbf{K}^* = \sum_{j=1}^{N_e}\mathbf{K}_j^*$, one obtains the damage index as follows:

$$MEBI_{ij} = \frac{(1-\alpha_j)\boldsymbol{\phi}_i^{*T}\mathbf{K}_j\boldsymbol{\phi}_i^*}{\omega_i^{*2}\boldsymbol{\phi}_i^{*T}\mathbf{M}\boldsymbol{\phi}_i^*} + \frac{\boldsymbol{\phi}_i^{*T}\mathbf{M}_j\boldsymbol{\phi}_i^*}{\boldsymbol{\phi}_i^{*T}\mathbf{M}\boldsymbol{\phi}_i^*} - \frac{\boldsymbol{\phi}_i^T\mathbf{K}_j\boldsymbol{\phi}_i}{\omega_i^2\boldsymbol{\phi}_i^T\mathbf{M}\boldsymbol{\phi}_i} - \frac{\boldsymbol{\phi}_i^T\mathbf{M}_j\boldsymbol{\phi}_i}{\boldsymbol{\phi}_i^T\mathbf{M}\boldsymbol{\phi}_i} \tag{13}$$

Because the severity of damage of each member is unknown, the damage index given by Eq. (13) cannot be calculated. There are two ways to solve this problem. Firstly, most of scholars (Stubbs *et al.* 1995, Srinivas *et al.* 2011, Seyedpoor 2012, Vo-Duy *et al.* 2016, Kaveh and Zolghadr 2017, Dinh-Cong *et al.* 2019b, Wang and Xu 2019) adopt the approximate hypothesis that only a few elements are damaged in practice, and these damages will make little difference for the overall MSE and MKE. Under this assumption, the severity of damage of each element equals to zero and the MEBI is reduced to

$$MEBI_{ij} = \frac{\boldsymbol{\phi}_i^{*T}\mathbf{K}_j\boldsymbol{\phi}_i^*}{\omega_i^{*2}\boldsymbol{\phi}_i^{*T}\mathbf{M}\boldsymbol{\phi}_i^*} + \frac{\boldsymbol{\phi}_i^{*T}\mathbf{M}_j\boldsymbol{\phi}_i^*}{\boldsymbol{\phi}_i^{*T}\mathbf{M}\boldsymbol{\phi}_i^*} - \frac{\boldsymbol{\phi}_i^T\mathbf{K}_j\boldsymbol{\phi}_i}{\omega_i^2\boldsymbol{\phi}_i^T\mathbf{M}\boldsymbol{\phi}_i} - \frac{\boldsymbol{\phi}_i^T\mathbf{M}_j\boldsymbol{\phi}_i}{\boldsymbol{\phi}_i^T\mathbf{M}\boldsymbol{\phi}_i} \tag{14}$$

If N_m modes are available, the MEBI can be written as

$$MEBI_j = \frac{1}{N_m}\sum_{i=1}^{N_m} MEBI_{ij} \tag{15}$$

The other way to solve the problem is the iterative damage localization index, which is effective but has been rarely investigated so far (Xu *et al.* 2019). It is found in Eq. (13) that if the damage severity $\boldsymbol{\alpha}$ has been estimated by an optimization algorithm, the MEBI can be constructed for damage localization. In return, if the damage locations has been predicted by the MEBI, $\boldsymbol{\alpha}$ can be re-estimated by the optimization algorithm. This is a cyclical process of structural damage identification. The MEBI can be accordingly written as an iterative form:

$$\left(MEBI_{ij}\right)^{[k]} = \frac{1}{N_m}\sum_{i=1}^{N_m}\left(\frac{\left(1-\alpha_j\right)^{[k-1]}\boldsymbol{\phi}_i^{*T}\mathbf{K}_j\boldsymbol{\phi}_i^*}{\omega_i^{*2}\boldsymbol{\phi}_i^{*T}\mathbf{M}\boldsymbol{\phi}_i^*} + \frac{\boldsymbol{\phi}_i^{*T}\mathbf{M}_j\boldsymbol{\phi}_i^*}{\boldsymbol{\phi}_i^{*T}\mathbf{M}\boldsymbol{\phi}_i^*} - \frac{\boldsymbol{\phi}_i^T\mathbf{K}_j\boldsymbol{\phi}_i}{\omega_i^2\boldsymbol{\phi}_i^T\mathbf{M}\boldsymbol{\phi}_i} - \frac{\boldsymbol{\phi}_i^T\mathbf{M}_j\boldsymbol{\phi}_i}{\boldsymbol{\phi}_i^T\mathbf{M}\boldsymbol{\phi}_i}\right) \tag{16}$$

where the square brackets $[k]$ used here is to indicate the k-th iteration. The z-score normalized index used to identify damage is obtained by

$$\left(nMEBI_{ij}\right)^{[k]} = \frac{\left(MEBI_{ij}\right)^{[k]} - \mu_{\left(MEBI_{ij}\right)^{[k]}}}{\sigma_{\left(MEBI_{ij}\right)^{[k]}}} \tag{17}$$

where $\mu_{(MEBI_{ij})^{[k]}}$ and $\sigma_{(MEBI_{ij})^{[k]}}$ are the sample mean and standard deviation, respectively, of the collection of $\left(MEBI_{ij}\right)^{[k]}$. The larger the value of the damage index is, the greater likelihood exists that the damage would occur. Given a threshold $nMEBI_t$, the element is determined as damaged if $\left(nMEBI_{ij}\right)^{[k]} > nMEBI_t$. In this study, this iterative MEBI given by Eq. (17) is used for damage localization.

2.2 BAS algorithm for damage quantification

After the damaged elements have been ascertained by the iterative MEBI, the damage severity of these elements can be estimated by an optimization algorithm. Due to the robust performance on general optimization problem, meta-heuristic optimization algorithms have been widely used, one of which is the BAS algorithm inspired by the searing behavior of longhorn beetles (Jiang and Li 2017). Compared with other swarm intelligence optimization algorithms (Kennedy and Eberhart 1995, Dorigo and Di Caro 1999, Karaboga and Basturk 2008), only one individual is required to search the best solution and the computational burden is greatly reduced.

In this study, the BAS algorithm is selected as the optimization algorithm for estimating the severity of damage, in which a beetle represents a predicted damage severity vector $\boldsymbol{\alpha} = \{\alpha_1, \alpha_2, \ldots, \alpha_{N_d}\}$ for the suspiciously damaged elements. In order to quantify the damage, a beetle needs to be (randomly) initialized, and this is actually a process, during which a damaged structure is assumed beforehand. The aim of the BAS optimization is searching a damaged structure corresponding to the smallest objective function among all the predicted damaged structures, namely, finding a damage severity vector α minimizing the defined objective function.

The process to estimate the severity of damage by the BAS algorithm is given in Algorithm 1, in which the operators *rnd*(•) and *sign*(•) denote the random and sign functions, and the sensing diameter d^0 and step size δ^0 are set as 0.01 and 0, respectively. Note that totally 500 iterations are executed in the BAS optimization process in the following study.

Algorithm 1 BAS for damage detection

Define objective function $f(\boldsymbol{\alpha})$, and $\boldsymbol{\alpha} = \{\alpha_1, \alpha_2, \ldots, \alpha_{N_d}\}$

Initialize the position $\boldsymbol{\alpha}^0$, the sensing diameter d^0, the step size δ^0, and the maximum number of iteration T_{max}

While $t \le T_{max}$ ***do***

Generate the direction vector unit $\boldsymbol{b}$ according to $\boldsymbol{b} = rnd(1, N_d)/\|rnd(1, N_d)\|$

Search in variable space with the left and right antennae according to $\boldsymbol{\alpha}_l = \boldsymbol{\alpha}^t - d^t\boldsymbol{b}, \boldsymbol{\alpha}_r = \boldsymbol{\alpha}^t + d^t\boldsymbol{b}$

Update the state variable $\boldsymbol{\alpha}^t$ according to $\boldsymbol{\alpha}^t = \boldsymbol{\alpha}^{t-1} + \delta^t\boldsymbol{b}sign(f(\boldsymbol{\alpha}_r - \boldsymbol{\alpha}_l))$

While $f(\boldsymbol{\alpha}^t) < f_{best}$ ***do***

Set $f_{best} = f(\boldsymbol{\alpha}^t), \boldsymbol{\alpha}_{best} = \boldsymbol{\alpha}^t$

Update d^t and δ^t with decreasing functions $d^t = 0.95d^{t-1} + d^0$ and $\delta^t = 0.95\delta^{t-1} + \delta^0$

End

End

For any optimization process, the objective function is crucial for searing the global optimal solution. Changes in natural frequencies, mode shapes, and their combinations were widely used in previously studies (Kim *et al.* 2003, Perera *et al.* 2009, Meruane and Heylen 2011, Xu *et al.* 2015, Shabbir and Omenzetter 2016, Frigui *et al.* 2018). The natural frequency is easily measured and had a strong effect on damage (Hakim and Razak 2013), and its measurement error is negligible in comparison to that in the mode shape (Perera *et al.* 2009). However, the spatial information of the structure cannot be reflected in the natural frequency (Yan *et al.* 2007).

The objective function based on their combination seems promising. Here the modal energy based objective function is established by using the natural frequency and mode shape information

$$f(\boldsymbol{\alpha}) = max\{|MEBI_1^{\sim}|, \ldots, |MEBI_j^{\sim}|, \ldots, |MEBI_{N_d}^{\sim}|\} \quad (18)$$

$$\begin{aligned} MEBI_j^{\sim} = \frac{1}{N_m}\sum_{i=1}^{N_m}\Bigg(&\frac{\widetilde{\boldsymbol{\phi}}_i^{*T}\mathbf{K}_j\widetilde{\boldsymbol{\phi}}_i^*}{\widetilde{\omega}_i^{*2}\widetilde{\boldsymbol{\phi}}_i^{*T}\mathbf{M}\widetilde{\boldsymbol{\phi}}_i^*} + \frac{\widetilde{\boldsymbol{\phi}}_i^{*T}\mathbf{M}_j\widetilde{\boldsymbol{\phi}}_i^*}{\widetilde{\boldsymbol{\phi}}_i^{*T}\mathbf{M}\widetilde{\boldsymbol{\phi}}_i^*} \\ &- \frac{\boldsymbol{\phi}_i^{*T}\mathbf{K}_j\boldsymbol{\phi}_i^*}{\omega_i^{*2}\boldsymbol{\phi}_i^{*T}\mathbf{M}\boldsymbol{\phi}_i^*} - \frac{\boldsymbol{\phi}_i^{*T}\mathbf{M}_j\boldsymbol{\phi}_i^*}{\boldsymbol{\phi}_i^{*T}\mathbf{M}\boldsymbol{\phi}_i^*}\Bigg) \end{aligned} \quad (19)$$

Note that $\widetilde{\omega}_i^*$ and ω_i^* are the *i*-th predicted and measured natural frequency, respectively; $\widetilde{\boldsymbol{\phi}}_i^*$ and $\boldsymbol{\phi}_i^*$ are the *i*-th predicted and measured mode shapes, of the damaged structure. When the predicted modal parameters equals the measured ones, $f(\boldsymbol{\alpha}) = 0$; otherwise, $f(\boldsymbol{\alpha}) > 0$.

2.3 Flowchart of the ITSM

In this paper, an ITSM method for structural damage identification is developed, in which if the damage location is determined by the iterative MEBI, the severity of the damage is estimated by BAS algorithm. In return, after the severity of damage is acquired, the iterative MEBI is further updated for re-localization.

Algorithm 2 ITSM for damage detection

Step (a): At iteration $k = 0$, $\boldsymbol{\alpha}^{[0]} = \{\alpha_1, \alpha_2, \ldots, \alpha_{N_e}\} = \mathbf{0}$

Step (b): Damage localization is performed by substituting $\boldsymbol{\alpha}^{[0]}$, ω_i^* and spatially complete mode shape $\boldsymbol{\phi}_i^*$ into Eq. (16). The group of the suspiciously damaged elements are arranged into a group $\boldsymbol{D}^{[1]} = \{e_1^*, e_2^*, \ldots, e_{D_1}^*\}$. Note that Guyan expansion (Guyan 1965) is used to acquire the spatially complete mode shape $\boldsymbol{\phi}_i^*$.

Step (c): The damage severity of $\boldsymbol{D}^{[1]}$ is estimated by the BAS algorithm to obtain the damaged severity vector $\boldsymbol{\alpha}^{[1]} = \{\alpha_1, \alpha_2, \ldots, \alpha_{D_1}\}$.

Step (d): At iteration $k = k + 1$, calculate the $\widetilde{\omega}_i^*$ and $\widetilde{\boldsymbol{\phi}}_i^*$ by performing an eigen-analysis for the predicted damaged structure, i.e, $(\widetilde{\mathbf{K}}^* - \widetilde{\omega}_i^{*2}\mathbf{M})\widetilde{\boldsymbol{\phi}}_i^* = \mathbf{0}$, where $\widetilde{\mathbf{K}}^* = \sum_{j=1}^{N_d}(1-\alpha_d)\mathbf{K}_d + \sum_{j=1}^{N_u}\mathbf{K}_u$; N_d and N_u are the predicted number of the damaged and undamaged elements at iteration $(k-1)$, and $N_d + N_u = N_e$; $\mathbf{K}_d$ and $\mathbf{K}_u$ are the stiffness matrices of the *d*-th and *u*-th elements, respectively, of the damaged structure.

Step (e): Damage localization is performed by substituting $\boldsymbol{\alpha}^{[k-1]}$, $\widetilde{\omega}_i^*$, $\widetilde{\boldsymbol{\phi}}_i^*$ and into Eq. (16) to obtain suspiciously damaged elements $\boldsymbol{D}^{[k]} = \{e_1^*, e_2^*, \ldots, e_{D_k}^*\}$.

Step (f): The damage severity of $\boldsymbol{D}^{[k]}$ is estimated to obtain $\boldsymbol{\alpha}^{[k]} = \{\alpha_1, \alpha_2, \ldots, \alpha_{D_k}\}$.

Step (g): Iteration continues by repeating the **Steps (d)** to **(f)** unless the convergence condition is achieved.

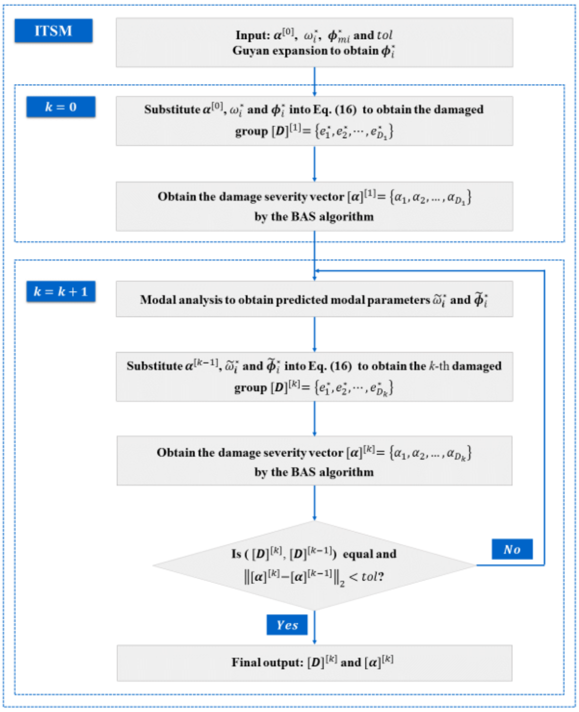

Fig. 1 Flowchart for the ITSM

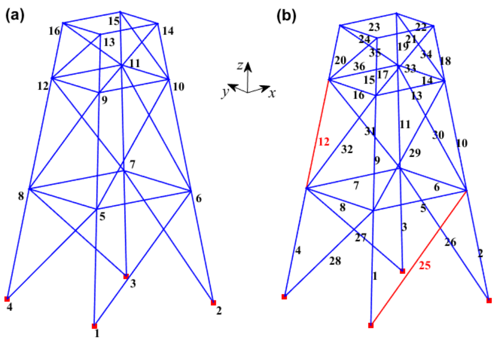

(a) nodes (b) elements

Fig. 2 Sketches of the 4-leg offshore platform structure

3. Numerical simulation

3.1 Description of the frame structure

The convergence condition is that the predicted damaged elements are unchanged from iteration $(k-1)$ to k and for each damaged element $\|\boldsymbol{\alpha}^{[k]} - \boldsymbol{\alpha}^{[k-1]}\|_2 < tol$, where $tol = 0.01\%$ is a preset threshold. For clarity, a flowchart of the ITSM is given in Fig. 1.

A simulated jacket platform structure is utilized in this study, as showed in Fig. 2. It comprises 36 steel pipe members, including 12 vertical legs (VL), 12 horizontal brace (HB), and 12 diagonal brace (DB) members. All VL, HB and DB members have uniform outer diameter of 11.55 cm and wall thickness of 2.00 cm, outer diameter of 9.15 cm and wall thickness of 1.50 cm and outer diameter of 6.75 cm and wall thickness of 1.20 cm, respectively. The height of the three stories is 9.00 m, 9.00 m and 4.50 m, and the side lengths of the bottom and top floors are 12.00×12.00 m and 5.75×4.75 m. The geometrical and material properties of the structure are as follows. For all the members, the elasticity modulus is 2.06×10^{11} N/m^2, the mass density is 7850 kg/m^3, and the Poisson ratio is 0.30. Executing an Eigen-analysis, one obtains the first three natural frequencies of the undamaged structure, i.e., 9.487 Hz, 9.669 Hz and 11.996 Hz, respectively. The first three mode shapes are displayed in Fig. 3, where the first two modes are bending modes vibrating in the horizontal direction, and the third mode is a torsional mode vibrating dominantly around z-direction.

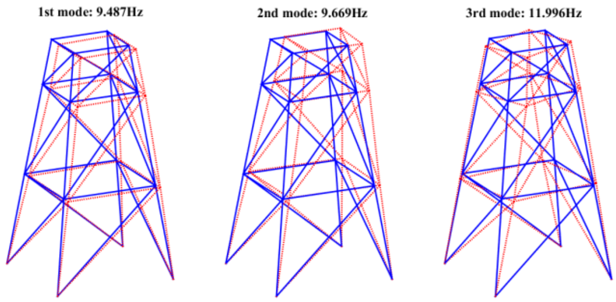

Fig. 3 The first three modes of the structure

3.2 Damage cases

The effects of measurement noise and spatial incompleteness of mode shape are considered. Both single- and double-damage cases are involved. The simulated damage cases are listed in Table 1.

When the effects of noise are considered, the measurements of the i-th polluted frequency and mode shape at the v-th degree of freedom (DoF) of the damaged structure, denoted by $\widehat{\omega}_i^*$ and $\widehat{\boldsymbol{\Phi}}_{vi}^*$ respectively, are simulated by adding a Gaussian random error to the corresponding true values:

$$\widehat{\omega}_i^* = \omega_i^*(1 + n_\omega \gamma_\omega) \tag{20}$$

$$\widehat{\boldsymbol{\Phi}}_{vi}^* = \boldsymbol{\Phi}_{vi}^*(1 + n_\phi \gamma_\phi) \tag{21}$$

where γ_ω and γ_ϕ are two Gaussian random numbers both with zero mean and unit standard deviation; n_ω and n_ϕ denote a modal noise level of natural frequency and mode shape, respectively. Messina *et al.* (1996) suggested a standard error of 0.15% as a benchmark for a natural frequency, and mode shape estimates have error levels as much as 20 times worse than those in the frequency estimates. Thus a standard error of 0.15% ($n_\omega = 0.15\%$) for the natural frequencies and 3% ($n_\phi = 3\%$) for the mode shapes are introduced to investigate the robustness of the ITSM in this study.

3.3 Damage identification using ITSM

To verify the effectiveness of the ITSM for structural damage identification, three damage scenarios are considered in this section. In each scenarios, only the first

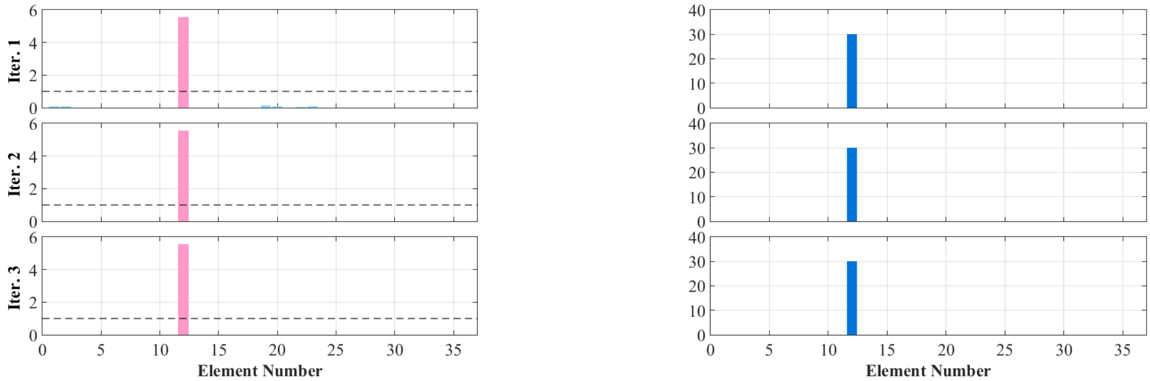

(a) damage index (b) severity of damage (%)

Fig. 4 Damage identification results of damage case A by the ITSM

Table 1 Damage cases simulated in the numerical study

Scenario	Case	Element	Severity	Natural frequency (Hz)		
				1st	2nd	3rd
Noise-free and spatially complete	A	12	30%	9.482	9.615	11.963
	B	25	30%	9.298	9.492	11.777
	C	12	30%	9.396	9.497	11.819
		25	20%			
Noise-polluted and spatially complete	D	12	30%	9.484	9.630	11.953
	E	25	30%	9.301	9.492	11.775
	F	12	30%	9.411	9.490	11.805
		25	20%			
Noise-polluted and spatially incomplete	G	12	30%	9.489	9.620	11.971
	H	25	30%	9.293	9.497	11.771
	I	12	30%	9.405	9.507	11.822

three modes ($N_m = 3$) are used. The modal displacements of nodal points 5 to 16 are measured and only three translational DoFs are available at each nodal point. Thus, 36 DoFs ($N_f = 36$) can be utilized for the spatially incomplete scenario.

For the TSM, the selection of the threshold determines which elements are preliminarily regarded as damaged. If a big threshold is used, false-negative detection errors may occur due to the fact that the truly damaged elements that are not revealed in the stage of damage localization will not be re-assessed any longer in the stage of damage quantification. However, if a small threshold is used, more undamaged elements will be mistakenly regarded as damaged, which provides a challenge for the optimization process with regard to the computational expense and accuracy. Taken together, the threshold $nMEBI_t = 1$ is selected herein for the nMEBI.

3.3.1 Noise-free and spatially complete scenario

Damage case A is a 30% damage occurring on the VL member 12. Fig. 4 shows the convergence history of damage localization and quantification. Note that the ITSM starts from $\boldsymbol{\alpha}^{[0]} = \mathbf{0}$ following the flowchart as given in Fig. 1. Based on the nMEBI, the most suspiciously damaged element is arranged as the initial damaged group $\boldsymbol{D}^{[1]} = \{12\}$. Then the initial estimation of damage severity is performed by the BAS algorithm. It is observed from Fig. 4(b) that the element 12 is with a 30.01% damage severity. Although the identified result in the first iteration is very close to the true damage state, the process of structural damage identification still needs to continue because the convergence condition is not achieved. In the second iteration, the nMEBI is updated based on the estimates of damage severity in the first iteration and then the damage is re-localized to obtain the new damaged group. The new group $\boldsymbol{D}^{[2]} = \{12\}$ is determined as the new damaged group as shown in Fig. 4(a). After three iterations of the ITSM, there is no change in the location and severity of damage. The final result shown in the bottom panels of Fig. 4 illustrates that the ITSM can identify the single damage in a noise-free and spatially complete scenario. Similar results are obtained in damage cases B and C. It is concluded that the ITSM is effective in identifying single- and double-damage in a noise-free and spatially complete environment.

3.3.2 Noise-polluted and spatially complete scenario

Fig. 5 shows the results of damage localization and quantification for damage case D in noise-polluted and spatially complete scenario. As showed in Fig. 5(a), the most potentially damaged elements include the truly damaged element 12 and the other undamaged element 30. Using the BAS algorithm to estimate the damage severity of the two elements, the estimates are 31.49% (true value 30%) and 4.26% (true value 0%) at elements 12 and 30. Then these two elements are retained for further damage localization. At the second iteration, element 12 is pointed out and arranged as the damaged group $\boldsymbol{D}^{[2]} = \{12\}$ for the estimation of severity, whereas the false positive of damage at element 30 is excluded. The variable space is narrowed from initial 2 to 1. After three iterations of the ITSM process, the convergence condition is achieved. The final result of damage identification is element 12 with a 31.55% (relative error 5.17%) stiffness loss, as shown in Fig. 5(b).

Performing damage detection analysis for damage cases E and F, one obtains the damage identification results, as

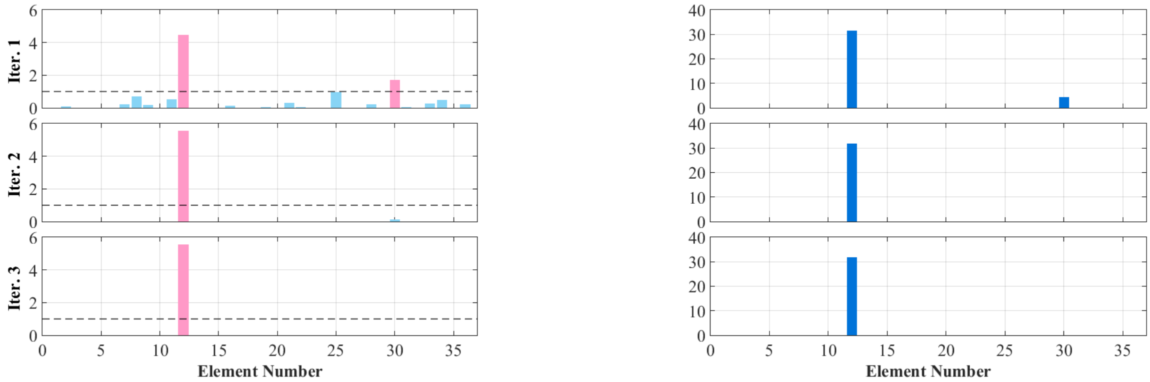

(a) damage index (b) severity of damage (%)

Fig. 5 Damage identification results of damage case D by the ITSM

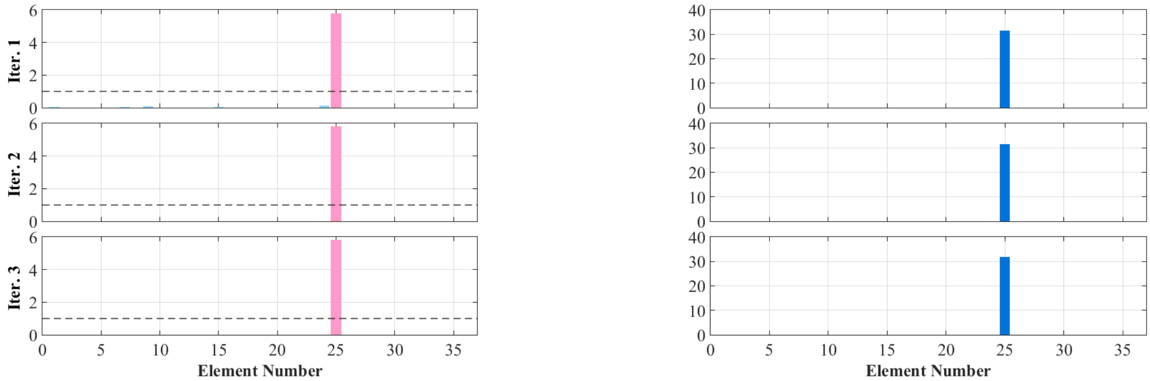

(a) damage index (b) severity of damage (%)

Fig. 6 Damage identification results of damage case E by the ITSM

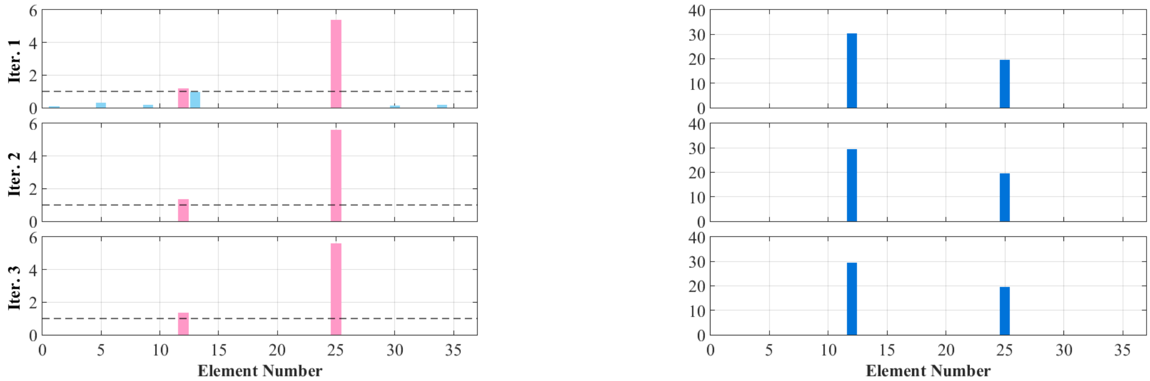

(a) damage index (b) severity of damage (%)

Fig. 7 Damage identification results of damage case F by the ITSM

showed in Figs. 6 and 7. For both damage cases, three iterations are run to achieve convergence, and only the truly damaged elements without any false positive errors are identified. For example, the damage severity estimates are 29.32% (true value 30%) at element 12, 19.32% (true value 20%) at element 25, respectively, for damage case F, both agreeing with the preset values. It is concluded that the ITSM accurately locates the damage and excludes the false-positive detection errors, and the precision of damage severity estimation is obviously improved.

3.3.3 Noise-polluted and spatially incomplete scenario

Table 2 shows the damage identification results for damage cases G to I in noise-polluted and spatially incomplete scenario. For damage case G, the most potentially damaged elements include the truly damaged element 12 and the other undamaged elements {23, 25-26} as showed in Table 2. Using the BAS algorithm to estimate the damage severity of these elements, the estimates are 48.94% (true value 30%) at element 12, 8.13% (true value

Table 2 Damage identification results of damage cases G to I by the ITSM

Case	True damage state		Estimated state			
	location	severity	location	Iter.1 severity	Iter.2 severity	Iter.3 severity
G	12	30	12	48.94%	30.51%	30.51%
			23	8.13%		
			25	0.91%		
			26	0.40%		
H	25	30%	25	34.85%	34.84%	34.84%
I	12	30%	12	34.33%	34.22%	34.22%
	25	20%	25	18.81%	18.82%	18.82%

0%) at element 23, 0.91% (true value 0%) at element 25, and 0.40% (true value 0%) at element 26, respectively at the first iteration. After three iterations of the ITSM process, the convergence condition is achieved. The final result of damage identification is element 12 with a 30.51% (relative error 1.70%) stiffness loss. Compared with that of the non-iterative method, the ITSM accurately locates the damage and excludes the false-positive detection errors, and the precision of damage severity estimation of the truly damaged location is obviously improved. For damage cases H and I, the nMEBI accurately locates the true damages in the first damage localization. Consequently, the ITSM fast identifies the damage severity under noise-polluted and spatially incomplete environment.

Furthermore, the damage missing error (DME) proposed by (Meruane and Mahu 2014) is used to investigate the effectiveness of the proposed ITSM under the noise-polluted and spatially incomplete conditions. Fig. 8 shows the DME of different type of element. For the VL (E12), the result of the obtained DME shown in Fig. 8(a) suggests that the correct identification ratio of the structural damage with less than 20% is extremely unsatisfied. More specially, 94% of the damage with severities 10% and 90% of the damage with severities 20% are undetected. However, the ITSM can identify the damage with severity larger than 30% with enough accuracy. For the DB (E25), the result of DME suggests that the ITSM can accurately identify the damage with severity larger than 10%. This difference confirms that the ITSM is more capable of identifying the damage at a diagonal brace than a vertical leg brace.

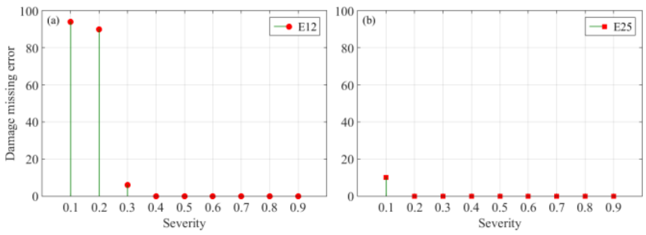

(a) VL (b) DB

Fig. 8 DME of different type of element

3.4 A comparison with other methods

3.4.1 Damage localization index

Considerable attention has been focused on Seyedpoor's MSEBI (Vo-Duy *et al.* 2016, Dinh-Cong *et al.* 2019b) due to its effectiveness for damage localization, it is, therefore, adopted as a counterpoint in this study to the proposed MEBI. Different with the MSEI given by Eq. (14), Seyedpoor's MSEBI only involves the structural MSE and is given as

$$MEEBI_{ij} = max[\mathbf{0}, \frac{(\boldsymbol{\phi}_i^{*T}\mathbf{K}_j\boldsymbol{\phi}_i^{*})/(\boldsymbol{\phi}_i^{*T}\mathbf{K}\boldsymbol{\phi}_i^{*})}{(\boldsymbol{\phi}_i^{T}\mathbf{K}_j\boldsymbol{\phi}_i)/(\boldsymbol{\phi}_i^{T}\mathbf{K}\boldsymbol{\phi}_i)} - 1] \qquad (22)$$

Similarly, the z-score normalized damage index of $MEEBI_{ij}$ can be constructed according to Eq. (17) and the element is determined as damaged if $nMSEBI_j > nMSEBI_t$. The threshold $nMSEBI_t = 1$ is selected herein for the MSEBI. In this section, the performance of the MEBI and MSEBI are compared.

Fig. 9 shows the damage localization results of noise-free and spatially complete scenario. Damage case A is a 30% damage occurring on the VL member 12. The nMSEBI can locate the truly damaged element 12 and other 4 undamaged elements, i.e. elements {28-29, 31-32}. In comparison, the nMEBI can accurately locate the true damage without any false-positive detection errors. This shows that the nMEBI has a better damage localization performance than the nMSEBI. The same conclusion that can be drawn from damage cases B and C.

Under noise-polluted scenario (see Fig. 10), it is evident that the nMEBI can successfully locate the actual damages with few false-positive errors, whereas the nMSEBI produces many false alarms, again, confirming that the nMEBI has a better damage localization performance than the nMSEBI.

The damage localization results turn bad for the noise-polluted and spatially incomplete scenario (see Fig. 11). For damage case G, the nMSEBI misses the truly damaged element 12 and mistakenly identified four undamaged elements. Similar results are found for damage cases H and I. In comparison, the nMEBI accurately locates the true damages even though produces few false-positive damage detection errors, thus is a better damage indicator. This shows an obvious improvement of the newly proposed index.

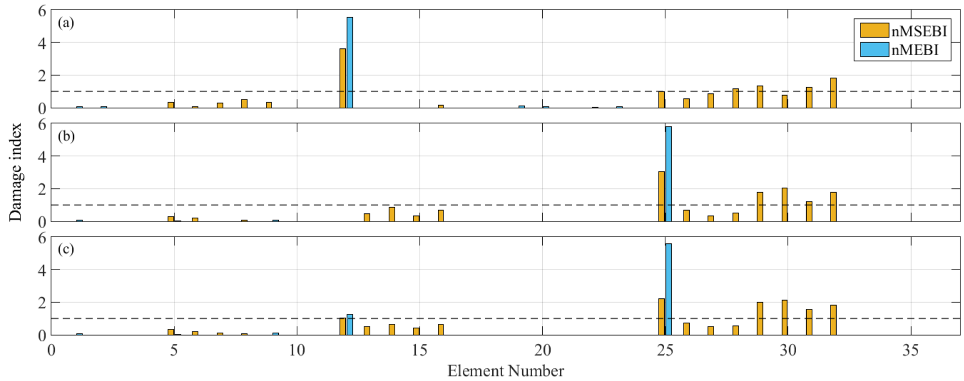

Fig. 9 Damage localization results under noise-free and spatially complete scenario of: (a) damage case A, (b) damage case B and (c) damage case C

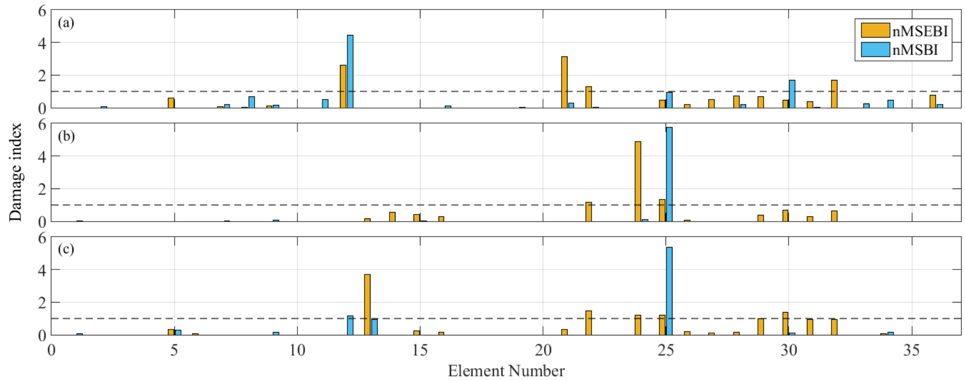

Fig. 10 Damage localization results under noise-polluted and spatially complete scenario of: (a) damage case D, (b) damage case E and (c) damage case F

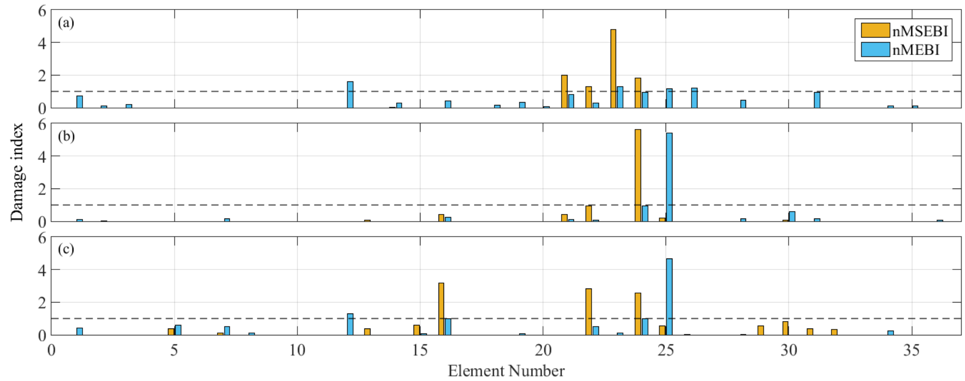

Fig. 11 Damage localization results under noise-polluted and spatially incomplete scenario of: (a) damage case G, (b) damage case H and (c) damage case I

3.4.2 Objective function

In this section, three objective functions based on the combination of the natural frequency and mode shape are compared to investigate the best performance of the ITSM.

(1) The modal flexibility based objective function (Pandey and Biswas 1994)

$$F_1 = \frac{1}{N_m}\sum_{i=1}^{N_m}\left(\|\widetilde{\boldsymbol{\phi}}_i^*\widetilde{\boldsymbol{\Lambda}}^*\widetilde{\boldsymbol{\phi}}_i^{*T} - \boldsymbol{\phi}_i^*\boldsymbol{\Lambda}^*\boldsymbol{\phi}_i^{*T}\|_2\right)^2 \tag{23}$$

where $\widetilde{\boldsymbol{\Lambda}}^*$ and $\boldsymbol{\Lambda}^*$ are the predicted and damaged diagonal matrix whose entities are $1/\widetilde{\omega}_i^{*2}$ and $1/\omega_i^{*2}$, respectively.

(2) The weighted objective function based on natural frequency and mode shape (Villalba and Laier 2012)

$$F_2 = \frac{1}{N_m}\sum_{i=1}^{N_m}\left(1 + \left|\frac{\widetilde{\omega}_i^* - \omega_i^*}{\omega_i^*}\right| + 2\sqrt{\frac{\sum_{m=1}^{N_f}\left(\widetilde{\phi}_{mi}^* - \phi_{mi}^*\right)^2}{\sum_{m=1}^{N_f}\left(\phi_{mi}^*\right)^2}}\right)^{-1} \tag{24}$$

where $\widetilde{\phi}_{mi}^*$ and ϕ_{mi}^* extracted from $\widetilde{\boldsymbol{\phi}}_i^*$ and $\boldsymbol{\phi}_i^*$ are the i-th predicted and measured mode displacements at the m-th DoFs, respectively; $\widetilde{\phi}_{mi}^*$ and ϕ_{mi}^* both with size of

Table 3 Identification results of damage cases D-F and I with different objective functions

Case	True damage state		Estimated state			
	location	severity	location	F_1 severity	F_2 severity	F_3 severity
D	12	30%	12	32.27%	32.36%	31.55%
E	25	30%	25	32.15%	32.22%	31.55%
F	12	30%	12			29.32%
	25	20%	25	27.79%	27.74%	19.32%
I	12	30%	12			34.18%
	25	20%	25	45.31%	22.66%	18.78%

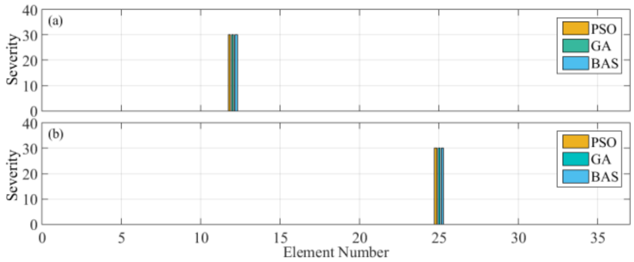

Fig. 12 Identification results with different algorithms of: (a) damage case A and (b) damage case B

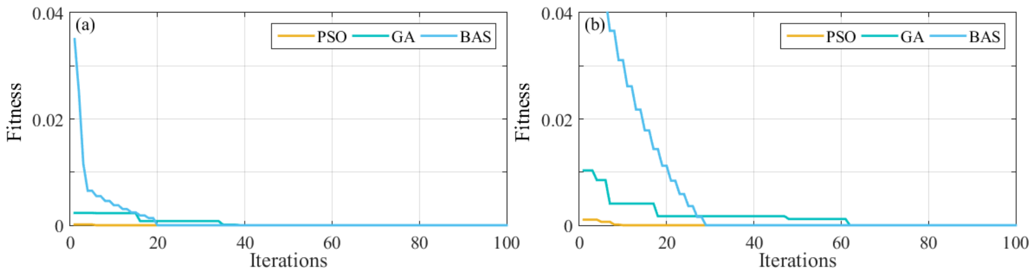

Fig. 13 Convergence history of different algorithms for: (a) damage case A and (b) damage case B

$N_f \times 1$ are the i-th predicted and measured mode shapes at N_f master DoFs of the damaged structure, respectively.

(3) The modal energy based objective function, i.e. the objective function given by Eq. (18).

The measurement noise and spatially incomplete mode shape are both considered here. Two single-damage cases (cases D and E) and two double-damage cases (cases F and I) are used to investigate the performance of the ITSM. A comparison of the damage identification results associated with three objective functions are listed in Table 3 for clarity.

It is realized from the results of the single-damage cases D and E that the damage on true-damaged elements can be identified by using each of the objective function. F_1 and F_2 estimate the damage severity with larger relative errors. By comparison, F_3 accurately determines the health state of all elements and has the best performance.

Results of damage cases F and I show that truly damaged element 12 is both missed when using F_1 and F_2, which indicates those objective functions are not good at locating damage. Besides, the estimate of the truly damaged element 25 is bad with great relative errors when using F_1 and F_2. Using the ITSM with F_1, the identified damage severity of the element 25 is 45.31% with more than 100% relative error in damage case I. By comparison, F_3 has the best performance with the most accurate damage localization information and the highest precision of damage severity estimation. It is concluded that the modal energy based objective function is more suitable for structural damage identification than the flexibility and the weighted objective function based on natural frequency and mode shape.

3.4.3 Objective function

In this section, the performance of the BAS algorithm is compared with those of other well-known optimization algorithms, namely the PSO (Kennedy and Eberhart 1995) and GA (Holland 1973). One uses 50 particles and 50 chromosomes for the PSO and the GA, respectively, while only one beetle for the BAS. For comparison, the maximum number of iteration is same for these three optimization algorithms, i.e. 100 iterations as shown in following study. Figs. 12 to 14 show the comparison associated with three

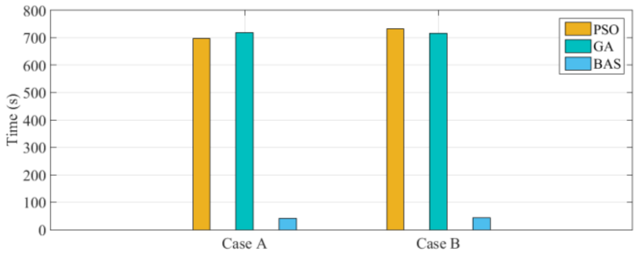

Fig. 14 Computational time of different algorithms for damage cases A and B

optimization algorithms. All these three algorithms can accurately locate and quantify the damage, as shown in Fig. 12. Fig. 13 displays the convergence history of different algorithms. It is indicated that the convergence speed of the BAS is significantly faster than the GA, but slower than the PSO. Further, Fig. 14 compares the computational time between the BAS and other two optimization algorithms and shows that the computational time of the BAS is approximately one-sixteenth of the PSO and the GA. In total, the BAS algorithm is more effective in solving the damage identification problem with great accuracy and low computational cost.

4. Experimental validation

4.1 Experimental setup

To evaluate the validity of the ITSM for damage identification, a cantilever beam structure (Wang and Li 2012) was experimentally tested. The beam had length of 200 cm, width of 5 cm and thickness of 2.8 cm. It was welded to base foundation at the bottom end with the other end free, as shown in Fig. 15(a). Twenty equal Euler-Bernoulli beam elements were used to simulate the beam, as shown in Fig. 15(b).

Acceleration responses were measured at seven nodal points 2/5/8/11/14/17/20 of the beam with seven accelerators. The sensor was Model 2220-005 of SILICON DESIGNS with an operating frequency from 0 to 600 Hz, and an amplitude rate of 5 g. All vibration signals were collected by the dynamic data acquisition system of CRONOS PL16-DCB8 for analysis. Throughout the modal test, a shock excitation on the beam was generated by means of an impulse hammer. To generate a maximum amplitude of vibration signal, the impact location was always selected at the free end of the beam.

Three cases were considered in the experiment. The experiment started by measuring the dynamic responses of the healthy beam. Then, a crack was generated to a desired depth using a saw cut (about 1 mm thickness) along the width direction. The cut location was 44.2 cm away from the clamped end, almost at the middle of element 16; the cut depth was 7 mm on one single side, about 1/4 of the beam thickness in the first damage case. Damage case II had a half depth cut with the same location as damage case I. The third damage case simulated a double-damage case, where both elements 16 and 7 (about 65.8 cm from the free end) had a half depth cut. In each case, the dynamic responses of the cracked beam were measured for modal identification and damage detection. During the dynamic testing, the measurement data was sampled at a sampling frequency of 200 Hz. The acceleration signals from the seven sensors were processed by the Eigen-system realization algorithm (Wang and Liu 2010) to obtain the natural frequencies and mode shapes. The first three natural frequencies of the damaged and the healthy structures in the experiment were listed in Tables 4 and 5.

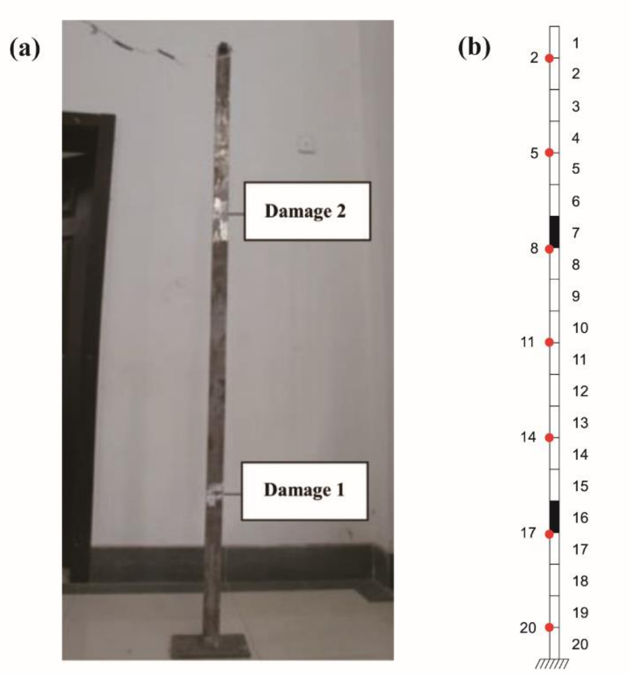

(a) physical model (b) FEM

Fig. 15 Cantilever beam structure used in the experiment

Table 4 Three damage cases simulated in the experiment

Case	Element	Cut depth (mm)	Natural frequency (Hz)		
			1st	2nd	3rd
D-I	16	7	5.473	34.768	96.874
D-II	16	14	5.299	34.755	95.089
D-III	7	14	5.289	33.837	91.485
	16	14			

Table 5 FREs and REFs of the healthy structure and finite element model

Model	Factor	1st	2nd	3rd
Healthy	FREs (Hz)	5.524	34.711	97.200
FEM	FREs (Hz)	5.586	35.005	98.016
	REFs (%)	1.12	0.85	0.84
Updated	FREs (Hz)	5.535	34.685	97.120
	REFs (%)	0.20	0.07	0.08

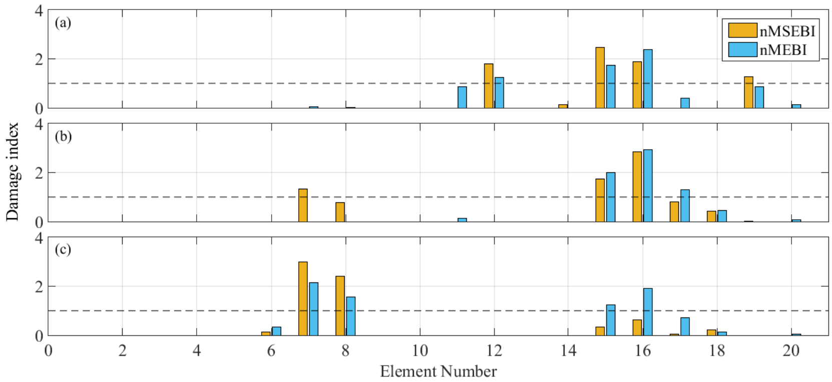

Fig. 16 Damage localization results in the experimental validation of: (a) damage case I, (b) damage case II and (c) damage case III

Table 6 Damage identification results of damage cases I to III among different objective function

Case	True damage state		Estimated state					
	location	cut depth	F_1 location	F_1 severity	F_2 location	F_2 severity	F_3 location	F_3 severity
D-I	16	7 mm	15	96.69%	16	19.92%	16	42.65%
D-II	16	14 mm	17	96.84%	16	49.08%	16	64.45%
D-III	7	14 mm			7	39.50%	7	59.85%
	16	14 mm	15	96.90%	15	50.94%	16	61.66%

4.2 Finite element model

A FEM was firstly constructed based on the physical parameter of the cantilever beam structure. The physical parameters of the FEM were as follows. The elasticity modulus was 2.06×10^{11} N/m^2, the mass density was 7850 kg/m^3. The first three natural frequencies (FREs) were 5.586 Hz, 35.005 Hz, and 98.016 Hz with the relative errors of frequencies (REFs) 1.12%, 0.85% and 0.84% to those of the healthy structure, respectively. The elasticity modulus and the mass density with the preset values were selected as the parameters for updating the FEM. This process was performed by using the response surface method (Ren and Chen 2010), and the updated values of the elasticity modulus and the mass density are 1.99×10^{11} N/m^2 and 7733.6 kg/m^3. By means of the model updating process, the first three REFs of the updated model and measured structure are reduced to 0.20%, 0.07%, and 0.08%, respectively, as listed in Table 5. It is indicated that the updated model has a good agreement to the measured structure. Thus the updated model was used as the numerical model of the cantilever beam.

4.3 Damage identification using ITSM

Throughout this experiment, the first three modes ($N_m = 3$) were identified. The modal displacements of nodal points 2/5/8/11/14/17/20 were measured and only one translational DoF was used to detect damage at each nodal point. The reduction method proposed by (Guyan 1965) was subsequently used for modal expansion to obtain the spatially complete mode shapes.

Firstly, a comparison of the damage localization results of the nMSEBI and nMEBI was performed with the experimental data, as shown in Fig. 16. For the small-damage case (D-I), the most like damage of the structure appears at element 15 with the maximum value of the nMSEBI. It means that the damage index nMSEBI misses the truly damaged element 16. On the contrary, the proposed index nMEBI can accurately locate the actual damage of structure. The same conclusion can be obtained from the double-damage case (D-III). Therefore, that the proposed nMEBI is superior to the other index in localizing the structural damage.

A detailed comparison of the damage identification results with regard to F_1, F_2, and F_3 was considered by using the proposed ITSM with the nMEBI. The ITSM with F_3 can accurately locate the actual damage of the structure while with other functions F_1 and F_2 cannot. Thus, the proposed modal energy-based objective function is superior to other two functions. It is worth mentioning that the performances of the ITSM with regard to damage severity estimation are not discussed here. This is because the true stiffness reduction in the beam is difficult to quantify on account of experimental errors.

5. Conclusions

An ITSM combining the MEBI with the BAS algorithm was proposed for structural damage identification. In each iteration, the MEBI was proposed to help effectively locate the potential damaged elements in the first stage, then the damage severity of these damaged elements was estimated in the second stage by minimizing an objective function with the BAS algorithm. The BAS algorithm was used is because it is fast and sufficient accurate of calculation. A modal energy based objective function was proposed. Numerical and experimental data were used to investigate the performance of the ITSM. The effects of measurement noise and spatial incompleteness of mode shape were both considered. The following conclusions are drawn:

- The proposed MEBI has a better performance than the MSEBI in damage localization.
- Based on the numerical simulation, the ITSM can identify single or multiple damage(s) in a noise-free environment. The ITSM can exclude the false-positive detection errors and accurately locate damages in a noise-polluted environment. Moreover, the precision of severity estimation is greatly improved because the false-positives occurring at the initial iteration are excluded.
- The modal energy based objective function is best adapted for the ITSM than the flexibility and the weighted objective function based on natural frequency and mode shape.

Note that the proposed ITSM is dependent on the precision of the numerical model. Using the model updating techniques such as the response surface-based approach, one can effectively obtain the numerical model for the laboratory structures. However, it is still a big challenge to obtain the accurate FEM of the complex and large-scale civil engineering structures with much more realistic uncertainties. The development of effective model updating techniques or the non-model damage detection methods are both in great demand.

Acknowledgments

The research described in this paper was financially supported by the National Science Fund for Distinguished Young Scholars (51625902), the National Key Research and Development Program of China (2019YFC0312404), the Major Scientific and Technological Innovation Project of Shandong Province (2019JZZY010820), the National Natural Science Foundation of China (51809134), the Natural Science Foundation of Shandong Province (ZR2017MEE007), and the Taishan Scholars Program of Shandong Province (TS201511016).

References

Alamdari, M.M., Li, J. and Samali, B. (2015), "Damage identification using 2-D discrete wavelet transform on extended operational mode shapes", *Arch. Civ. Mech. Eng.*, **15**(3), 698-710. https://doi.org/10.1016/j.acme.2014.12.001.

Casciati, S. and Elia, L. (2017), "Damage localization in a cable-stayed bridge via bio-inspired metaheuristic tools", *Struct. Control. Health. Monit.*, **24**(5), e1922. https://doi.org/10.1002/stc.1922.

Cha, Y.J. and Buyukozturk, O. (2015), "Structural damage detection using modal strain energy and hybrid multi-objective optimization", *Comput-Aided. Civ. Inf.*, **30**(5), 347-358. https://doi.org/10.1111/mice.12122.

Chaabane, M., Mansouri, M., Ben Hamida, A., Nounou, H. and Nounou, M. (2019), "Multivariate statistical process control-based hypothesis testing for damage detection in structural health monitoring systems", *Struct. Control. Health. Monit.*, **26**(1), e2287. https://doi.org/10.1002/stc.2287.

Cornwell, P., Doebling, S.W. and Farrar, C.R. (1999), "Application of the strain energy damage detection method to plate-like structures", *J. Sound. Vib.*, **224**(2), 359-374. https://doi.org/10.1006/jsvi.1999.2163.

Dessi, D. and Camerlengo, G. (2015), "Damage identification techniques via modal curvature analysis: overview and comparison", *Mech. Syst. Signal. Pr.*, **52**, 181-205. https://doi.org/10.1016/j.ymssp.2014.05.031.

Dinh-Cong, D., Nguyen-Thoi, T., Vinyas, M. and Nguyen, D.T. (2019a), "Two-stage structural damage assessment by combining modal kinetic energy change with symbiotic organisms search", *Int. J. Struct. Stab. Dy.*, **19**(10), 1950120. https://doi.org/10.1142/S0219455419501207.

Dinh-Cong, D., Vo-Duy, T., Ho-Huu, V. and Nguyen-Thoi, T. (2019b), "Damage assessment in plate-like structures using a two-stage method based on modal strain energy change and Jaya algorithm", *Inverse. Probl. Sci. En.*, **27**(2), 166-189. https://doi.org/10.1080/17415977.2018.1454445.

Dinh-Cong, D., Vo-Duy T. and Nguyen-Thoi T. (2018), "Damage assessment in truss structures with limited sensors using a two-stage method and model reduction", *Appl. Soft. Comput.*, **66**, 264-277. https://doi.org/10.1016/j.asoc.2018.02.028.

Dinh-Cong, D., Vo-Van, L., Nguyen-Quoc, D. and Nguyen-Thoi T. (2019c), "Modal kinetic energy change ratio-based damage assessment of laminated composite beams using noisy and incomplete measurements", *J. Adv. Eng. Comput.*, **3**(3), 452-463. https://doi.org/10.25073/jaec.201933.248.

Dorigo, M. and Di Caro, G. (1999), "Ant colony optimization: a new meta-heuristic", *Proceedings of the 1999 Congress on Evolutionary Computation*, Washington, DC, USA, July.

Frigui, F., Faye, J.P., Martin, C., Dalverny, O., Pérès, F. and Judenherc, S. (2018), "Global methodology for damage detection and localization in civil engineering structures", *Eng. Struct.*, **171**, 686-695. https://doi.org/10.1016/j.engstruct.2018.06.026.

Ghiasi, R. and Ghasemi, M.R. (2018). "An intelligent health monitoring method for processing data collected from the sensor network of structure", *Steel. Compos. Struct.*, **29**(6), 703-716. https://doi.org/10.12989/scs.2018.29.6.703.

Guyan, R.J. (1965), "Reduction of stiffness and mass matrices", *AIAA. J.*, **3**(2), 380. https://doi.org/10.2514/3.2874.

Hakim, S.J.S. and Razak, H.A. (2013), "Structural damage detection of steel bridge girder using artificial neural networks and finite element models", *Steel. Compos. Struct.*, **14**(4), 367-377. https://doi.org/10.12989/scs.2013.14.4.367.

Hu, S.L.J., Wang, S.Q. and Li, H.J. (2006), "Cross-modal strain energy method for estimating damage severity", *J. Eng. Mech.*, **132**(4), 429-437. https://doi.org/10.1061/(ASCE)0733-9399(2006)132:4(429).

Holland, J. (1973), "Genetic algorithms and the optimal allocation of trials", *SIAM. J. Comput.*, **2**(2), 88-105. https://doi.org/10.1137/0202009.

Jiang, X.Y. and Li, S. (2017), "BAS: beetle antennae search algorithm for optimization problems", *arXiv preprint*, arXiv: 1710.10724. https://doi.org/10.5430/ijrc.v1n1p1.

Kang, F., Li, J.J. and Xu, Q. (2012), "Damage detection based on improved particle swarm optimization using vibration data", *Appl. Soft. Comput.*, **12**(8), 2329-2335. https://doi.org/10.1016/j.asoc.2012.03.050.

Karaboga, D. and Basturk, B. (2008), "On the performance of artificial bee colony (ABC) algorithm", *Appl. Soft. Comput.*,

8(1), 687-697. https://doi.org/10.1016/j.asoc.2007.05.007.

Kaveh, A. and Zolghadr, A. (2017), "Cyclical Parthenogenesis Algorithm for guided modal strain energy based structural damage detection", *Appl. Soft. Comput.*, **57**, 250-264. https://doi.org/10.1016/j.asoc.2017.04.010.

Kennedy, J. and Eberhart, R. (1995), "Particle swarm optimization", *Proceedings of IEEE International Conference on Neural Networks*, **4**, 1942-1948. https://doi.org/10.1109/ICNN.1995.488968.

Kim, J.T., Ryu, Y.S., Cho, H.M. and Stubbs, N. (2003), "Damage identification in beam-type structures: frequency-based method vs mode-shape-based method", *Eng. Struct.*, **25**(1), 57-67. https://doi.org/10.1016/S0141-0296(02)00118-9.

Li, H.J., Fang, H. and Hu, S.L.J. (2007), "Damage localization and severity estimate for three-dimensional frame structures", *J. Sound. Vib.*, **301**(3-5), 481-494. https://doi.org/10.1016/j.jsv.2006.08.042.

Meruane, V. and Heylen, W. (2011), "An hybrid real genetic algorithm to detect structural damage using modal properties", *Mech. Syst. Signal. Pr.*, **25**(5), 1559-1573. https://doi.org/10.1016/j.ymssp.2010.11.020.

Meruane, V. and Mahu, J. (2014), "Real-time structural damage assessment using articial neural networks and antiresonant frequencies", *Shock. Vib.*, **2014**, 1-14. https://doi.org/10.1155/2014/653279.

Messina, A., Jones, I.A. and Williams, E.J. (1996), "Damage detection and localization using natural frequency changes", *Proceedings of Conference on Identification in Engineering Systems*, Swansea, UK, March.

Nobahari, M., Ghasemi, M.R. and Shabakhty, N. (2017), "Truss structure damage identification using residual force vector and genetic algorithm", *Steel. Compos. Struct.*, **25**(4), 485-496. https://doi.org/10.12989/scs.2017.25.4.485.

Oliveira, G., Magalhães, F., Cunha, Á. and Caetano, E. (2018), "Vibration-based damage detection in a wind turbine using 1 year of data", *Struct. Control. Health. Monit.*, **25**, e2238. https://doi.org/10.1002/stc.2238.

Pandey, A.K. and Biswas, M. (1994), "Damage detection in structures using changes in flexibility", *J. Sound. Vib.*, **169**(1), 3-17. https://doi.org/10.1006/jsvi.1994.1002.

Pandey, A.K., Biswas, M. and Samman, M.M. (1991), "Damage detection from changes in curvature mode shapes", *J. Sound. Vib.*, **145**(2), 321-332. https://doi.org/10.1016/0022-460X(91)90595-B.

Perera, R., Fang, S.E. and Huerta, C. (2009), "Structural crack detection without updated baseline model by single and multi-objective optimization", *Mech. Syst. Signal. Pr.*, **23**(3), 752-768. https://doi.org/10.1016/j.ymssp.2008.06.010.

Ren, W.X. and Chen, H.B. (2010), "Finite element model updating in structural dynamics by using the response surface method", *Eng. Struct.*, **32**(8), 2455-2465. https://doi.org/10.1016/j.engstruct.2010.04.019.

Seyedpoor, S.M. (2012), "A two stage method for structural damage detection using a modal strain energy based index and particle swarm optimization", *Int. J. Nonlin. Mech.*, **47**(1), 1-8. https://doi.org/10.1016/j.ijnonlinmec.2011.07.011.

Shabbir, F. and Omenzetter, P. (2016), "Model updating using genetic algorithms with sequential niche technique", *Eng. Struct.*, **120**, 166-182. https://doi.org/10.1016/j.engstruct.2016.04.028.

Shi, Z.Y., Law, S.S. and Zhang, L.M. (1998), "Structural damage localization from modal strain energy change", *J. Eng. Mech.*, **218**(5), 825-844. https://doi.org/10.1006/jsvi.1998.1878.

Shirazi, M.N., Mollamahmoudi, H. and Seyedpoor, S.M. (2014), "Structural damage identification using an adaptive multi-stage optimization method based on a modified particle swarm algorithm", *J. Optimiz. Theory. App.*, **160**(3), 1009-1019. https://doi.org/10.1007/s10957-013-0316-6.

Srinivas, V., Ramanjaneyulu, K. and Jeyasehar, C.A. (2011), "Multistage approach for structural damage identification using modal strain energy and evolutionary optimization techniques", *Struct. Health. Monit.*, **10**(2), 219-230. https://doi.org/10.1177/1475921710373291.

Stubbs, N., Kim, J.T. and Farrar, C.R. (1995), "Field verification of a nondestructive damage localization and severity estimation algorithm", *Proceedings of the International Modal Analysis Conference*, Bethel, Conn, USA, February.

Tang, H., Zhang, W., Xie, L. and Xue, S. (2013), "Multi-stage approach for structural damage identification using particle swarm optimization", *Smart. Struct. Syst.*, **11**(1), 69-86. https://doi.org/10.12989/sss.2013.11.1.069.

Tiachacht, S., Bouazzouni, A., Khatir, S., Wahab, M.A., Behtani, A. and Capozucca, R. (2018), "Damage assessment in structures using combination of a modified Cornwell indicator and genetic algorithm", *Eng. Struct.*, **177**, 421-430. https://doi.org/10.1016/j.engstruct.2018.09.070.

Villalba, J.D. and Laier, J.E. (2012), "Localizing and quantifying damage by means of a multi-chromosome genetic algorithm", *Adv. Eng. Softw.*, **50**, 150-157. https://doi.org/10.1016/j.advengsoft.2012.02.002.

Vo-Duy, T., Ho-Huu, V., Dang-Trung, H. and Nguyen-Thoi, T. (2016), "A two-step approach for damage detection in laminated composite structures using modal strain energy method and an improved differential evolution algorithm", *Compos. Struct.*, **147**, 42-53. https://doi.org/10.1016/j.compstruct.2016.03.027.

Wang, S.Q. and Li, H.J. (2012), "Assessment of structural damage using natural frequency changes", *Acta. Mech. Sin.*, **28**(1), 118-127. https://doi.org/10.1007/s10409-012-0017-7.

Wang, S.Q., Li, H.J. and Hu, S.L.J. (2009), "Cross modal strain energy method for damage localization and severity estimation", *Proceedings of the 26th International Conference on Offshore Mechanics and Arctic Engineering*, San Diego, California, USA, June.

Wang, S.Q. and Liu, F.S. (2010), "New accuracy indicator to quantify the true and false modes for eigensystem realization algorithm", *Struct. Eng. Mech.*, **34**(5), 625-634. https://doi.org/10.12989/sem.2010.34.5.625.

Wang, S.Q., Wang, H.Y. and Xu, M.Q. (2020), "Identifying the presence of structural damage: a statistical hypothesis testing approach combined with residual strain energy", *Mech. Syst. Signal. Pr.*, **140**, 106655. https://doi.org/10.1016/j.ymssp.2020.106655.

Wang, S.Q. and Xu, M.Q. (2019), "Modal strain energy-based structural damage identification: a review and comparative study", *Struct. Eng. Int.*, **29**(2), 234-248. https://doi.org/10.1080/10168664.2018.1507607.

Wang, S.Q., Xu, M.Q., Xia, Z.P. and Li, Y.C. (2019), "A novel Tikhonov regularization-based iterative method for structural damage detection of offshore platforms", *J. Mar. Sci. Tech.*, **24**(2), 575-592. https://doi.org/10.1007/s00773-018-0579-6.

Xu, Y., Qian, Y., Song, G. and Guo, K. (2015), "Damage detection using finite element model updating with an improved optimization algorithm", *Mech. Syst. Signal. Pr.*, **19**(1), 191-208. https://doi.org/10.12989/scs.2015.19.1.191.

Xu, M.Q. and Wang, S.Q. (2017), "Cross modal strain energy-based structural damage detection in the presence of noise effects", *Adv. Mech. Eng.*, **9**(12). https://doi.org/10.1177/1687814017744122.

Xu, M.Q., Wang, S.Q. and Jiang, Y.F. (2019), "Iterative two-stage approach for identifying structural damage by combining the modal strain energy decomposition method with the multi-objective particle swarm optimization algorithm", *Struct. Control. Health. Monit.*, **26**(2), e2301. https://doi.org/10.1002/stc.2301.

Yan, Y.J., Cheng, L., Wu, Z.Y. and Yam, L.H. (2007), "Development in vibration based structural damage detection", *Mech. Syst. Signal. Pr.*, **21**(5), 2198-2211. https://doi.org/10.1016/j.ymssp.2006.10.002.

CC